



## Article

# Role of TiO<sub>2</sub> Nanoparticles in Wet Friction and Wear Properties of PEO Coatings Developed on Pure Titanium

Maryam Molaei <sup>1</sup>, Arash Fattah-Alhosseini <sup>1,\*</sup> , Meisam Nouri <sup>1</sup> and Mosab Kaseem <sup>2,\*</sup> <sup>1</sup> Department of Materials Engineering, Bu-Ali Sina University, Hamedan 65178-38695, Iran<sup>2</sup> Corrosion and Electrochemistry Laboratory, Department of Nanotechnology and Advanced Materials Engineering, Sejong University, Seoul 05006, Republic of Korea

\* Correspondence: a.fattah@basu.ac.ir (A.F.-A.); mosabkaseem@sejong.ac.kr (M.K.)

**Abstract:** The present study aims to explain how the incorporation of anatase TiO<sub>2</sub> nanoparticles at three different concentrations, i.e., 1, 3, and 5 g/L, into the ceramic-like oxide plasma electrolytic oxidation (PEO) coatings on pure titanium substrate can affect the friction and wear behavior of the coatings in simulated body fluid (SBF) aqueous solution. For this purpose, a ball-on-disk friction and wear tester was utilized to characterize the wear performance of the PEO coatings. The morphology and dimensions (width and depth) of wear tracks were analyzed by scanning electron microscopy (SEM) and 2D depth profilometry, respectively. The results indicated that abrasive wear was identified in all PEO coatings; however, the coefficient of friction (COF), wear volume loss, and wear rate were strongly affected by the concentration of TiO<sub>2</sub> nanoparticles. The coatings containing TiO<sub>2</sub> nanoparticles presented a lower COF, less wear volume loss, reduced wear rate, and improved wear resistance due to having smoother surfaces and the presence of hard TiO<sub>2</sub> nanoparticles on their surfaces and inside the pores. The coating with 3 g/L of TiO<sub>2</sub> nanoparticles demonstrated the lowest wear rate value of  $1.33 \times 10^{-6}$  mm<sup>3</sup>/Nm (about a 32% reduction compared with that of coating without TiO<sub>2</sub> nanoparticles) and the best wear protection properties among all coatings under investigation. The findings suggest TiO<sub>2</sub> nanoparticles incorporated PEO coatings as a promising choice of surface treatment wherein the load-bearing capacity of titanium implants is critical.

**Keywords:** TiO<sub>2</sub> nanoparticles; titanium; plasma electrolytic oxidation (PEO); wear; simulated body fluid (SBF)



**Citation:** Molaei, M.; Fattah-Alhosseini, A.; Nouri, M.; Kaseem, M. Role of TiO<sub>2</sub> Nanoparticles in Wet Friction and Wear Properties of PEO Coatings Developed on Pure Titanium. *Metals* **2023**, *13*, 821. <https://doi.org/10.3390/met13040821>

Academic Editors: Krzysztof Rokosz and Agnieszka Kułakowska

Received: 21 March 2023

Revised: 12 April 2023

Accepted: 19 April 2023

Published: 21 April 2023



**Copyright:** © 2023 by the authors. Licensee MDPI, Basel, Switzerland. This article is an open access article distributed under the terms and conditions of the Creative Commons Attribution (CC BY) license (<https://creativecommons.org/licenses/by/4.0/>).

## 1. Introduction

Titanium and its alloys are very popular in orthopedic and dental implant applications, owing to their suitable mechanical strength, corrosion resistance, and biocompatibility [1–3]. The excellent corrosion resistance of titanium is because of the natural oxide film of a few tens of nanometers that spontaneously forms over its surface upon exposure to air or moisture [4,5]. However, major problems with titanium and its alloys, which substantially confine their clinical performance in load-bearing implant applications, are their weak wear-resistance properties and high friction coefficient caused by damage to the thin and brittle oxide film that results in severe adhesive wear [3,4,6,7]. Wear of the implants releases significant amounts of metallic particles into the human body, causing local irritations or systemic issues and loosening of the implants which could result in their removal [8,9]. Therefore, to enhance the titanium implants' tribological properties and increase their long-term service life, proposals have included coating their surfaces using different surface modification techniques such as plasma electrolytic oxidation (PEO), physical vapor deposition (PVD), chemical vapor deposition (CVD), and plasma spray [8,10,11].

As a simple, efficient, and eco-friendly electrochemical process applied at high external potential, PEO is considered a promising method for modifying the surface of titanium and its alloys [12–14]. PEO ceramic-like oxide coatings are porous, hard, and thick, and

adhere well to the substrate, providing high resistance to corrosion and wear [15]. Moreover, the porous nature of the PEO coatings brings an opportunity for incorporating nano- or micro-sized particles such as SiC, TiO<sub>2</sub>, ZrO<sub>2</sub>, CeO<sub>2</sub>, and Al<sub>2</sub>O<sub>3</sub> added into the electrolyte into them, thereby enhancing the coatings' hardness and wear properties [16–20]. As an example, Shokouhfar et al. [18] found that the integration of SiC, Al<sub>2</sub>O<sub>3</sub>, and TiO<sub>2</sub> nanoparticles into the PEO coatings increased their surface hardness and reduced their surface roughness, coefficient of friction (COF), and wear rate (W). In another study, Xu et al. [21] concluded that the incorporation of SiO<sub>2</sub> nanoparticles into the PEO coating reduced COF and W values of the coating, because of the high hardness and self-lubricating properties of such particles, and eventually improved its tribological performance.

To date, scholars have mainly focused on the role of incorporated nano- or microparticles in PEO coatings on dry friction and wear properties of coatings and only a few studies have investigated the tribological behavior of these in wet and lubricating environments. This work aims to study the wear and friction characteristics of PEO oxide coatings formed on pure titanium substrate under the influence of anatase TiO<sub>2</sub> nanoparticles added into the electrolyte in simulated body fluid (SBF) solution, using the ball-on-disk technique. Accordingly, the surface microstructure and roughness, phase composition, COF, wear volume loss (V), and W values and also wear mechanism of the obtained PEO-coated specimens are investigated.

## 2. Materials and Methods

Commercial pure titanium (grade 2) 20 × 20 × 1 mm<sup>3</sup> plates were utilized as substrate material (anode). Samples were ground using SiC sandpapers, cleaned with ethanol, and then rinsed with distilled water before the coating process. The PEO treatment was conducted in pulsed direct current (DC) mode (PM700/7 PRC, IPS apparatus) in an aqueous electrolyte solution containing Na<sub>3</sub>PO<sub>4</sub>·12H<sub>2</sub>O, KOH, and Ca<sub>3</sub>(PO<sub>4</sub>)<sub>2</sub> without and with different concentrations of anatase TiO<sub>2</sub> nanoparticles. The average diameter of TiO<sub>2</sub> nanoparticles was 20 nm. Na<sub>3</sub>PO<sub>4</sub>·12H<sub>2</sub>O and KOH were used as agents for preparing an alkaline electrolyte and increasing the electrical conductivity of the electrolyte, respectively. Ca<sub>3</sub>(PO<sub>4</sub>)<sub>2</sub> is a biocompatible material that is used as a source of Ca and P, the two main compositional elements of human bone, in the PEO process electrolytes to prepare Ca-P coatings for biological applications [22]. The composition of the electrolytes used in this study is given in Table 1. A MIRA III TESCAN scanning electron microscope (SEM—made in Brno, Czech Republic) was used to record the image of the TiO<sub>2</sub> nanoparticles (see Figure 1). To disperse the TiO<sub>2</sub> nanoparticles in the electrolytes, we used an ultrasonic instrument. During the coating process, the electrolyte was continuously agitated by a magnetic stirrer and cooled with cold water to hold its temperature below 35 °C. The settings of the PEO process were as follows: 2000 Hz for the frequency of the pulse, 5 A/dm<sup>2</sup> for the current density, 30% for the duty ratio, and 5 min treatment time.

**Table 1.** The chemical composition of the PEO process electrolytes for each sample code.

Sample Code	Components (g/L)			
	Na <sub>3</sub> PO <sub>4</sub> ·12H <sub>2</sub> O	KOH	Ca <sub>3</sub> (PO <sub>4</sub> ) <sub>2</sub>	TiO <sub>2</sub> Nanoparticles
0-TiO <sub>2</sub>	5	3	1	0
1-TiO <sub>2</sub>	5	3	1	1
3-TiO <sub>2</sub>	5	3	1	3
5-TiO <sub>2</sub>	5	3	1	5

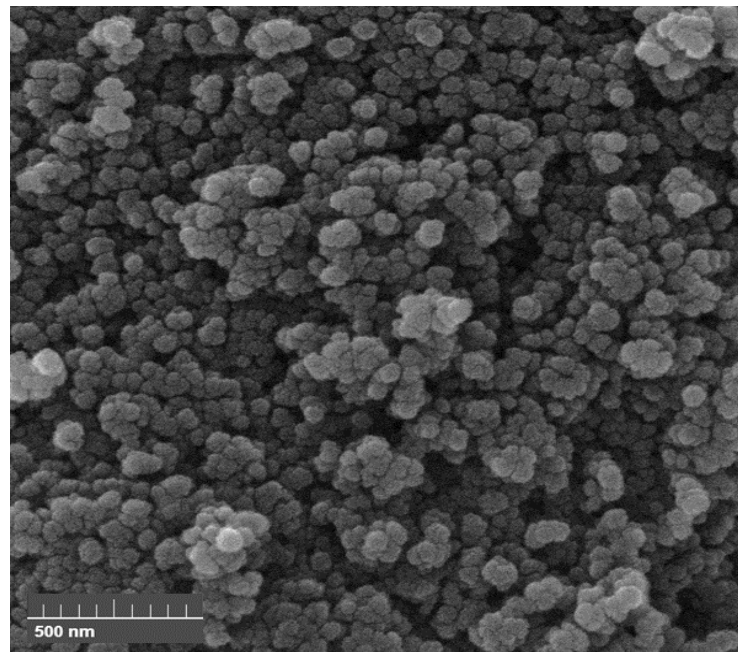


**Figure 1.** The SEM image of the anatase TiO<sub>2</sub> nanoparticles at a magnification of 100,000 $\times$ .

The PEO coatings' surface morphology was observed using the SEM images (captured by a QUANTA 200 FEI microscope, made in Hillsboro, OR, USA). The SEM images of the PEO coatings were further analyzed using Microstructural Image Processing (MIP) software in order to determine their average pore size and porosity percentage. The phase identification of the coatings was performed with an X-ray diffractometer (PHILIPS-PW1730 diffractometer equipped with a Cu K $\alpha$  source, operating at 40 kV and 30 mA with a step size of 0.05 $^\circ$ , made in Eindhoven, Netherlands). The quantitative analysis of the anatase and rutile TiO<sub>2</sub> phases of the PEO coatings was performed according to the Rietveld refinement method utilizing Material Analysis Using Diffraction (MAUD) software. The RT2200 PCE roughness tester (made in Meschede, Germany) was employed to measure the surface roughness of the PEO coatings. Each measurement was made 10 times on each side of the sample, and the obtained data were averaged.

The wear behavior of the PEO coatings was assessed using a ball-on-disk oscillating tribometer (Faragir Sanat Mehrbin, Isfahan, Iran) with a 5 N normal load, a rotation speed of 50 rpm, and a track diameter of 10 mm with a sliding distance of 50 m in SBF solution (pH = 7.4) at room temperature. The composition of the SBF solution is summarized in Table 2 [23]. Al<sub>2</sub>O<sub>3</sub> ceramic balls of 6 mm diameter were utilized as abrasive friction partners. During the experiments, the COF of the samples was recorded using a computer connected to the tribometer. To calculate the V of the samples, the wear profile was measured after each wear test with a 2D depth profilometer (Mitutoyo, SJ-210/310/410, made in Bangkok, Thailand). Then, the W corresponding to each PEO-coated sample was obtained using Equation (1) [24]:

$$W = V/PL \quad (1)$$

where V is the wear volume loss, P is the normal load, and L is the sliding distance. Each measurement was repeated 3 times for each PEO-coated sample. Finally, the morphology of the wear tracks was examined using SEM images.

**Table 2.** The chemical composition of SBF solution used in tribological tests.

Component	Amount
NaCl	8.035 g/L
NaHCO <sub>3</sub>	0.355 g/L
KCl	0.225 g/L
K <sub>2</sub> HPO <sub>4</sub> ·3H <sub>2</sub> O	0.231 g/L
MgCl <sub>2</sub> ·6H <sub>2</sub> O	0.311 g/L
1.0 <sub>M</sub> -HCl	39 mL
CaCl <sub>2</sub>	0.292 g/L
Na <sub>2</sub> SO <sub>4</sub>	0.072 g/L
Tris	6.118 g/L

### 3. Results and Discussions

#### 3.1. Surface Microstructure and Roughness of Coatings

The surface microstructure and roughness of the PEO coatings are among the important factors affecting the wear-resistance properties of the coatings. Figure 2 shows the surface microstructure of the PEO coatings without and with different concentrations of TiO<sub>2</sub> nanoparticles at low and high magnifications. It was observed that the surfaces of all coatings were characterized by micropores, as typical features of the PEO process [25,26], though the size, number, and shape of the micropores differed between each coating. According to the reported data in Table 3, the coating without TiO<sub>2</sub> nanoparticles possessed the lowest degree of porosity (2.17%) but the highest average pore size ( $1.42 \pm 0.75 \mu\text{m}$ ) among all the tested coatings. The addition of TiO<sub>2</sub> nanoparticles into the electrolyte reduced the surface porosity of the coatings from 5.73% to 2.28% due to the closure of many micropores. On the other hand, the average pore size of the coatings with TiO<sub>2</sub> nanoparticles decreased from  $1.38 \pm 0.72$  to  $1.00 \pm 0.63 \mu\text{m}$  as the concentration of TiO<sub>2</sub> nanoparticles was increased from 1 to 3 g/L, and then increased to  $1.27 \pm 0.71 \mu\text{m}$  with further addition of TiO<sub>2</sub> nanoparticles up to 5 g/L. This might have been caused by changes in the size and intensity of the sparks that occurred on the surface of the anode during the coating process with the increase in the concentration of TiO<sub>2</sub> nanoparticles in the electrolyte.

Additionally, tiny white nanoparticles (indicated by yellow arrows) and agglomerates of such particles could be seen over the surface and in the pores of the TiO<sub>2</sub> nanoparticles-containing coatings (see Figure 2c,e,g). It seems that most of the TiO<sub>2</sub> nanoparticles were spread over the surfaces rather than filling the pores. Having a zeta potential of  $-20.20 \text{ mV}$  in the PEO experimental alkaline electrolyte (with a pH of 12.46), the TiO<sub>2</sub> nanoparticles were charged negatively and then migrated toward the anode due to electrophoresis [27], and were successfully included in the coatings. With the addition of greater amounts of TiO<sub>2</sub> nanoparticles into the electrolyte, more nanoparticles entered the coatings. According to our previous study [28], adding TiO<sub>2</sub> nanoparticles into the electrolyte did not alter the coatings' thickness significantly (see Table 3).

Moreover, the PEO coatings that incorporated TiO<sub>2</sub> nanoparticles had lower surface roughness values (in the range of  $0.35 \pm 0.03$  to  $0.38 \pm 0.01 \mu\text{m}$ ) in comparison with the coating without TiO<sub>2</sub> nanoparticles (with a surface roughness value of  $0.52 \pm 0.03 \mu\text{m}$ ) (see Table 3). This may have resulted from the smaller micropores size and the trapping of some nanoparticles in the micropores of coatings with TiO<sub>2</sub> nanoparticles. However, there was no major dissimilarity between the surface roughness values of the PEO coatings prepared with the addition of different concentrations of TiO<sub>2</sub> nanoparticles into the electrolyte.



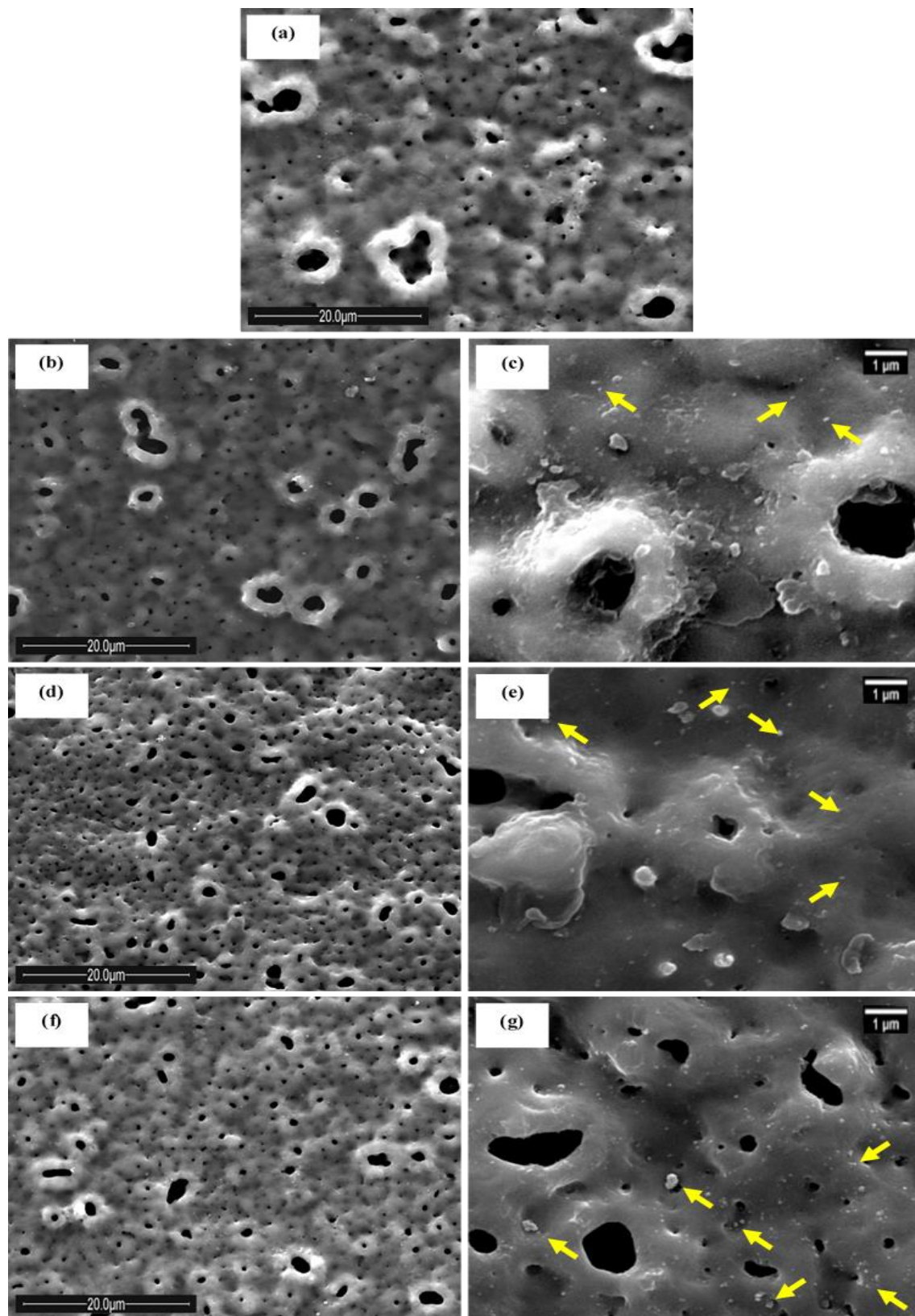


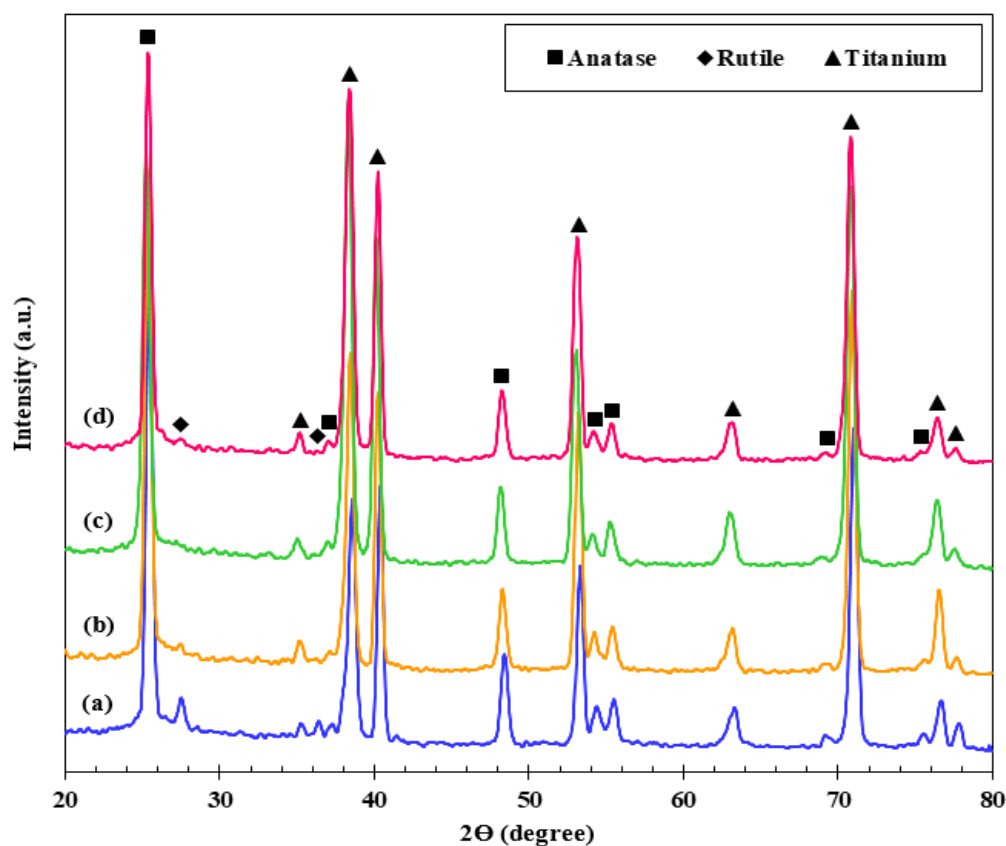
**Figure 2.** The surface morphologies of the PEO coatings (a) without and with (b,c) 1 g/L, (d,e) 3 g/L, and (f,g) 5 g/L of anatase TiO<sub>2</sub> nanoparticles at low and high magnifications (5000× and 20,000×, respectively).

**Table 3.** The average pore size, porosity percentage, surface roughness, and thickness values of the PEO coatings without and with different concentrations of anatase TiO<sub>2</sub> nanoparticles.

Sample	Average Pore Size ( $\mu\text{m}$ )	Porosity (%)	Roughness ( $\mu\text{m}$ )	Thickness ( $\mu\text{m}$ )
0-TiO <sub>2</sub>	$1.42 \pm 0.75$	2.17	$0.52 \pm 0.03$	$3.66 \pm 0.83$
1-TiO <sub>2</sub>	$1.38 \pm 0.72$	5.73	$0.35 \pm 0.03$	$3.75 \pm 0.86$
3-TiO <sub>2</sub>	$1.00 \pm 0.63$	2.50	$0.38 \pm 0.03$	$2.85 \pm 0.62$
5-TiO <sub>2</sub>	$1.27 \pm 0.71$	2.28	$0.38 \pm 0.01$	$2.70 \pm 0.75$

### 3.2. The Phase Identification of the Coatings

The XRD patterns of different PEO coatings are given in Figure 3. While the coating without TiO<sub>2</sub> nanoparticles contained anatase (reference code 00-002-0387) and a small amount of rutile (reference code 01-078-1510), as two major polymorphs of TiO<sub>2</sub>, the coatings with TiO<sub>2</sub> nanoparticles were mainly composed of anatase. The formation of rutile and anatase is due to the outward migration of titanium and the inward migration of oxygen at the metal–electrolyte interface [22,29]. Moreover, the peaks of the titanium substrate (reference code 00-001-1198) were mainly caused by the porosity and low thickness of the coatings within the penetration depth of the X-rays. According to the calculated mass fraction of anatase and rutile phases present in the coatings, as shown in Table 4, by increasing the concentration of TiO<sub>2</sub> nanoparticles in the electrolyte up to 3 g/L, the quantity of anatase decreased from 76.6 to 62.0 wt.%. However, it did not change further with addition of TiO<sub>2</sub> nanoparticles up to 5 g/L. Therefore, it was apparent that despite the increase in the concentration of TiO<sub>2</sub> nanoparticles in the electrolyte, the amount of anatase in coatings did not increase. Based on our previous study [28], Fourier-transform infrared spectroscopy (FTIR) analysis confirmed the presence of phosphate (PO<sub>4</sub><sup>3−</sup>) compounds in the coatings caused by the use of phosphate-based electrolytes in the PEO process.

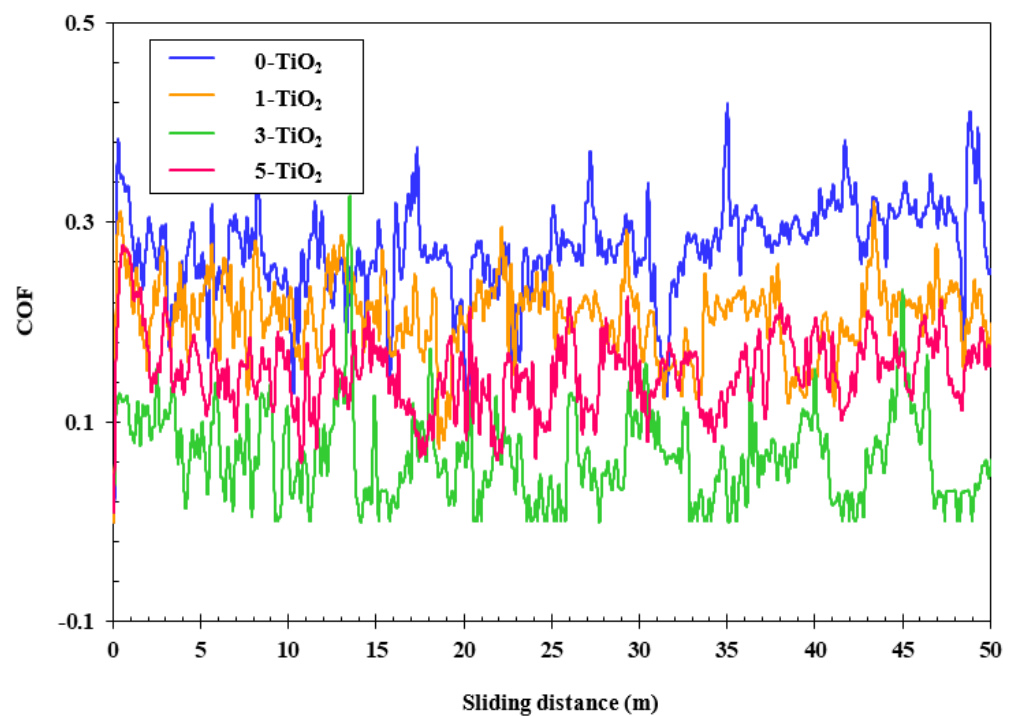
**Figure 3.** XRD patterns of the PEO coatings (a) without and with (b) 1 g/L, (c) 3 g/L, and (d) 5 g/L of anatase TiO<sub>2</sub> nanoparticles.

**Table 4.** The anatase and rutile phases' mass fraction of the PEO coatings without and with different concentrations of anatase TiO<sub>2</sub> nanoparticles.

Sample	Anatase (wt.%)	Rutile (wt.%)
0-TiO <sub>2</sub>	76.6	9.3
1-TiO <sub>2</sub>	74.6	1.7
3-TiO <sub>2</sub>	62.0	-
5-TiO <sub>2</sub>	63.5	1.0

### 3.3. Wear Behavior of the Coatings in SBF Solution

The COF curves in terms of the sliding distance and calculated average COF values of the PEO coatings without and with different concentrations of TiO<sub>2</sub> nanoparticles obtained by the ball-on-disk wear test with a load of 5 N and 50 m distance against an Al<sub>2</sub>O<sub>3</sub> ceramic ball in SBF solution are shown in Figures 4 and 5, respectively. As can be observed in Figure 4, a sharp increase in COF was observed in all curves at the beginning of the test. Piling up of wear debris on the wearing path and the rolling of fine particles over each other, in addition to cold bonding between the surfaces, led to fluctuations in the COF curves of all the PEO-coated samples. The coatings with TiO<sub>2</sub> nanoparticles showed smaller average COF values (in the range of 0.06 to 0.20) than the coating without TiO<sub>2</sub> nanoparticles (with an average COF value of 0.27). The reason for this can be traced back to the lower surface roughness values of the coatings with TiO<sub>2</sub> nanoparticles (see Table 3). The surface roughness of solid materials is an important factor that affects the contact stress, adhesion, and friction between two surfaces [30]. Similar results were obtained by Shokouhfar et al. [18]. Moreover, while the average COF value of coatings with TiO<sub>2</sub> nanoparticles initially decreased from 0.20 to 0.06 by incorporating TiO<sub>2</sub> nanoparticles up to 3 g/L, the extra addition of the TiO<sub>2</sub> nanoparticles up to 5 g/L resulted in an increase of the average COF value to 0.14.

**Figure 4.** The variation of the COF versus the sliding distance curves of different PEO coatings recorded during the ball-on-disk wear test in the SBF solution.

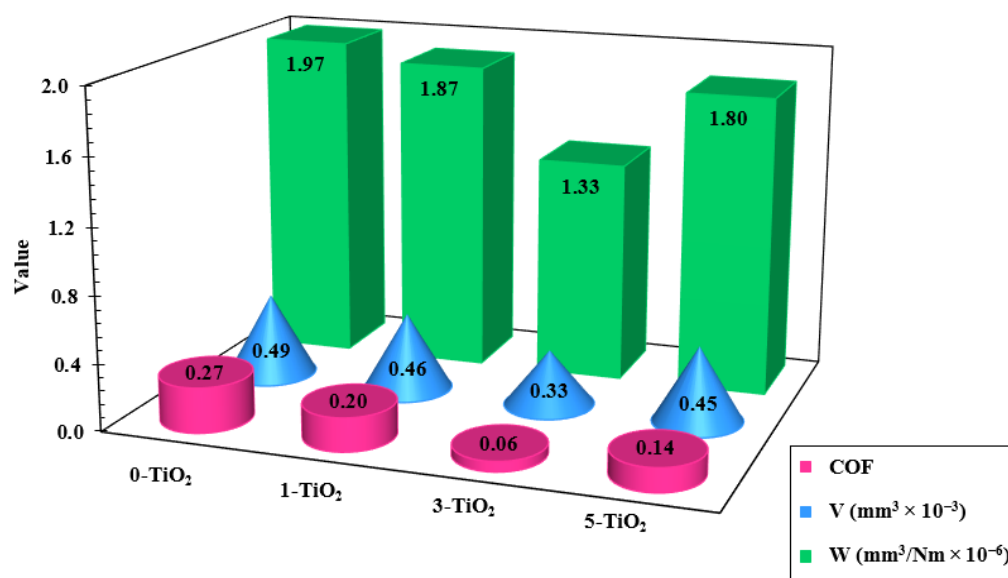


**Figure 5.** The variations of COF, V, and W values for four different coated specimens.

The electron microscopy images from the worn surfaces of the PEO-coated samples are exhibited in Figures 6 and 7. Due to the small thickness and the high brittleness of the PEO ceramic coatings, all coatings appeared to have been completely worn out. The titanium substrate under the coatings was plowed after sliding for 50 m. The worn surfaces mainly displayed plowed grooves parallel to the sliding direction with some detached wear debris, indicating a characteristic feature of the abrasive wear mechanism. According to the review paper by Guo et al. [31], while the wear behavior under dry friction conditions usually involves adhesive wear and material transfer, the liquid medium to a certain extent inhibits adhesive wear and material transfer. Therefore, it seems that the liquid SBF medium inhibited the adhesive wear in the coatings and the transfer of material from the Al<sub>2</sub>O<sub>3</sub> ceramic ball. It can be observed that the wear track on the surface of the PEO coatings with TiO<sub>2</sub> nanoparticles was narrower, smoother, and more uniform with noticeably less damage, compared with that on the surface of the coating without TiO<sub>2</sub> nanoparticles. The latter showed extensive delamination and plowing of the titanium substrate. Therefore, as was expected, the incorporation of TiO<sub>2</sub> nanoparticles into the coatings had a positive effect on the wear behavior.

The above observations were further supported by the 2D depth profiles of the coatings' wear tracks. According to Figure 8, the cross-sectional area of the wear track on the surface of the coating without TiO<sub>2</sub> nanoparticles (with measured width and depth of 1.21 mm and 24.47  $\mu\text{m}$ , respectively) was wider and deeper than that on the surfaces of coatings incorporating TiO<sub>2</sub> nanoparticles. Therefore, it can be concluded that the introduction of TiO<sub>2</sub> nanoparticles into the electrolyte effectively lowered the wear volume loss and wear rate values of the coatings from 0.49 to  $0.33 \times 10^{-3} \text{ mm}^3$  and 1.97 to  $1.33 \times 10^{-6} \text{ mm}^3/\text{Nm}$ , respectively, (see Figure 5), and thereby improved the coatings' wear resistance properties. Generally, the wear performance of PEO coatings can be affected by their mechanical properties (e. g. surface hardness), chemical composition, surface roughness and porosity, and thickness [20,30]. Accordingly, the better anti-wear properties of the coatings with TiO<sub>2</sub> nanoparticles may be attributed to the presence of hard TiO<sub>2</sub> ceramic nanoparticles on the surfaces and inside the pores as well as the lower surface roughness of the coatings. PEO coatings' wear resistance can be effectively enhanced with the addition of hard nanoparticles [20,32]. Moreover, PEO coatings with high surface roughness show an increased rate of wear [33,34].



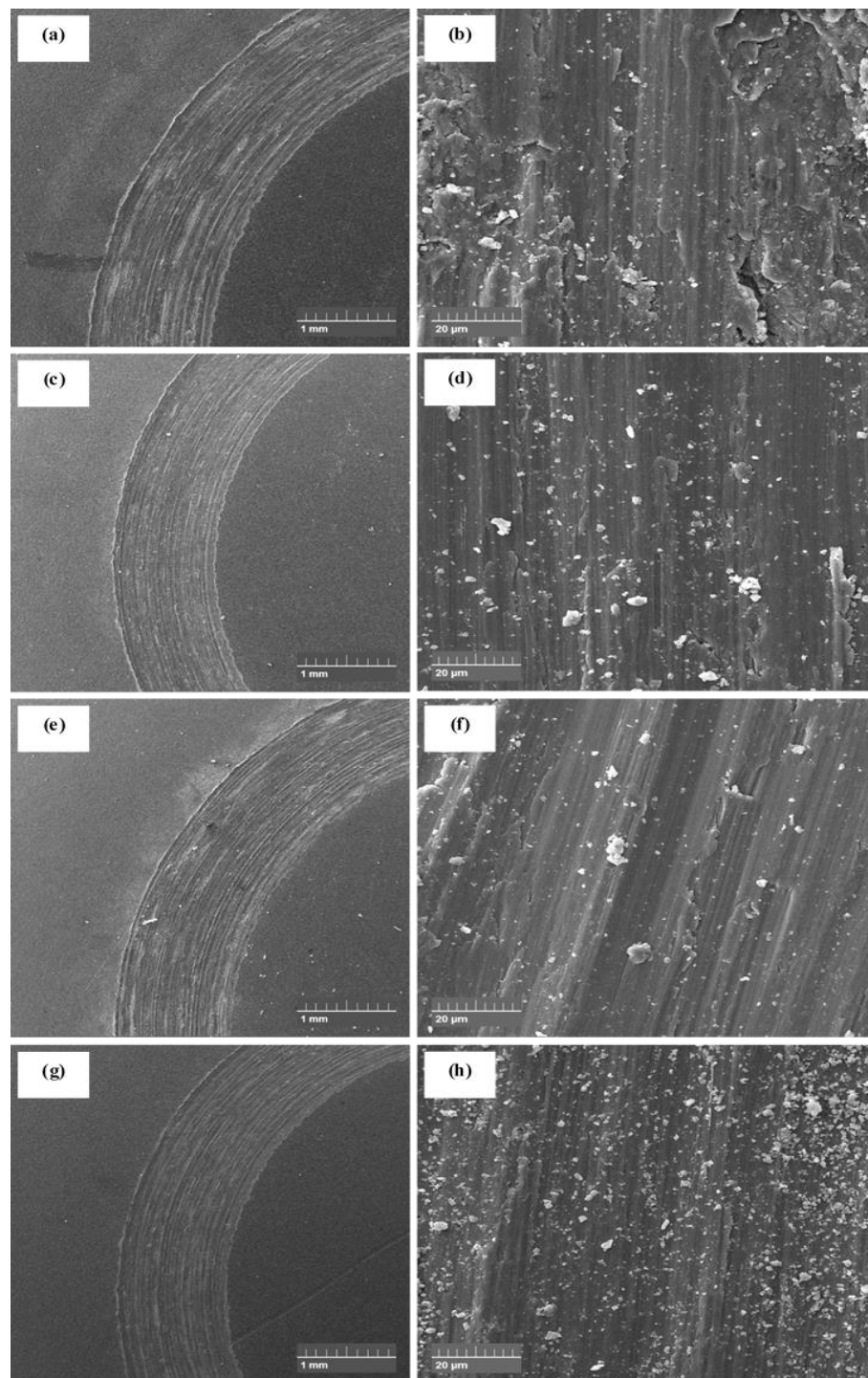


**Figure 6.** The wear tracks of the PEO coatings (a,b) without and with (c,d) 1 g/L, (e,f) 3 g/L, and (g,h) 5 g/L of anatase TiO<sub>2</sub> nanoparticles after the ball-on-disk wear test in SBF solution, viewed at magnifications of 50× and 2000×.

It is evident from Figure 8 that the width and depth of the wear tracks on the surfaces of the PEO coatings with TiO<sub>2</sub> nanoparticles decreased for different concentrations of the nanoparticles, in the following order: 1 and 5 g/L < 3 g/L and 3 g/L < 5 g/L < 1 g/L, respectively. Due to the incorporation of more TiO<sub>2</sub> nanoparticles and also the reduction of the size and content of the porosity, the wear performance of the coatings was enhanced by increasing the concentration of TiO<sub>2</sub> nanoparticles up to 3 g/L (see Figure 5). Porosities and pores may play a nocuous role in the tribological performance of PEO coatings because

they may cause the application of higher stresses to the outmost surfaces or could be initiation sites for cracks [35]. However, the addition of 5 g/L of  $\text{TiO}_2$  nanoparticles into the electrolyte had a detrimental effect on the wear resistance of the coating in terms of increasing the wear volume loss and wear rate (from  $0.33$  to  $0.45 \times 10^{-3} \text{ mm}^3$  and  $1.33$  to  $1.80 \times 10^{-6} \text{ mm}^3/\text{Nm}$ , respectively) (see Figure 5). This might be due to the increase in the average size of the pores after the addition of more  $\text{TiO}_2$  nanoparticles into the electrolyte. Aliofkhaei et al. [36] reported that lower amounts of nanoparticles distribute well and provide better anti-wear performance in coatings, due to the agglomeration of nanoparticles in the valleys of coatings that occurs at high concentrations. Therefore, the higher agglomeration of  $\text{TiO}_2$  nanoparticles at a concentration of 5 g/L might deteriorate the wear performance of the coating. The best wear protection properties were obtained in the coating with 3 g/L of  $\text{TiO}_2$  nanoparticles, leading to a reduction of about 32% in the wear rate value. Therefore, the wear-resistance properties of the PEO coatings were found to be dependent on the concentration of  $\text{TiO}_2$  nanoparticles.

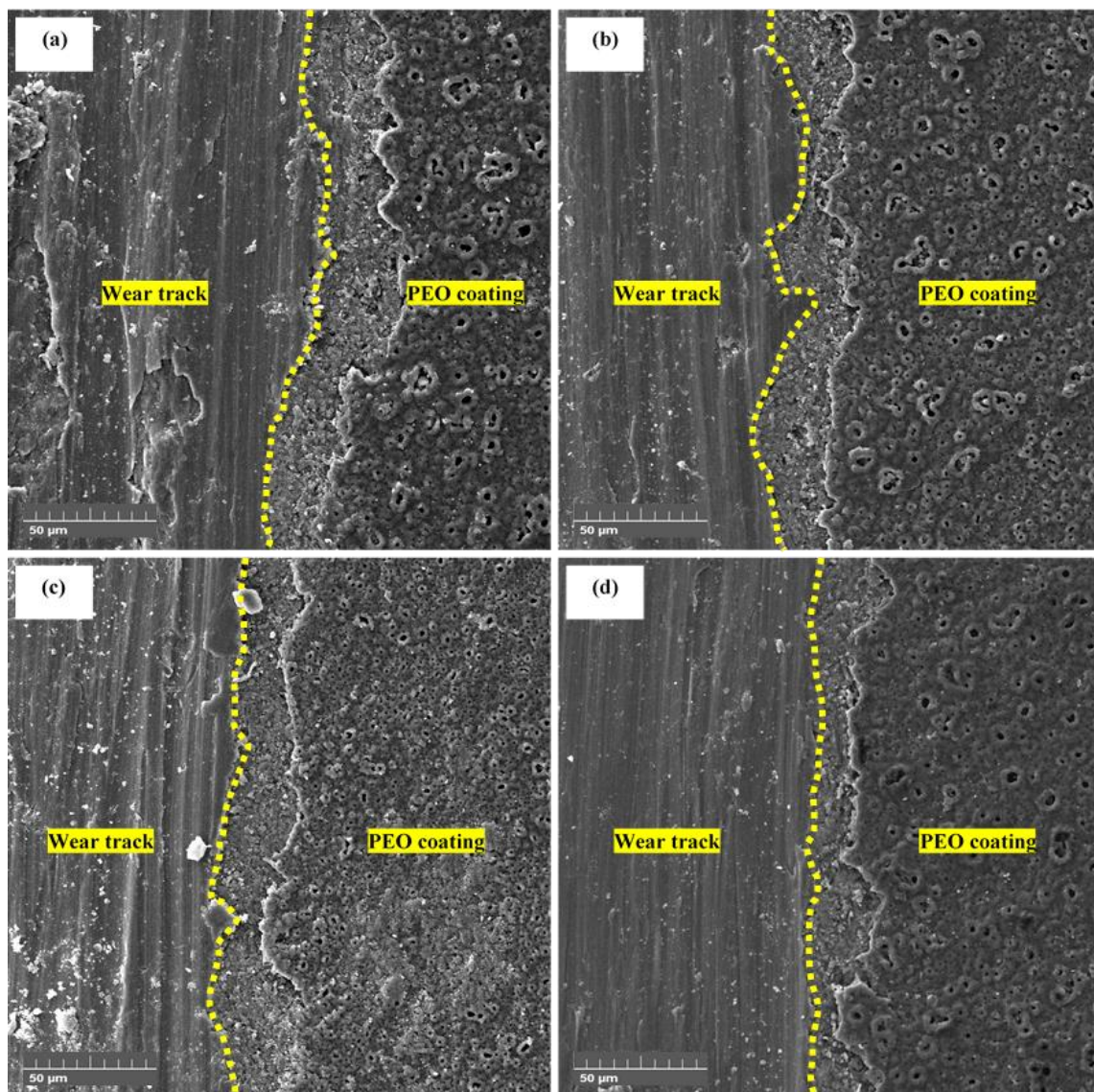


**Figure 7.** The interface morphology of worn and unworn surfaces of the PEO coatings (a) without and with (b) 1 g/L, (c) 3 g/L, and (d) 5 g/L of anatase  $\text{TiO}_2$  nanoparticles after the ball-on-disk wear test in SBF solution, viewed at a magnification of  $1000\times$ .

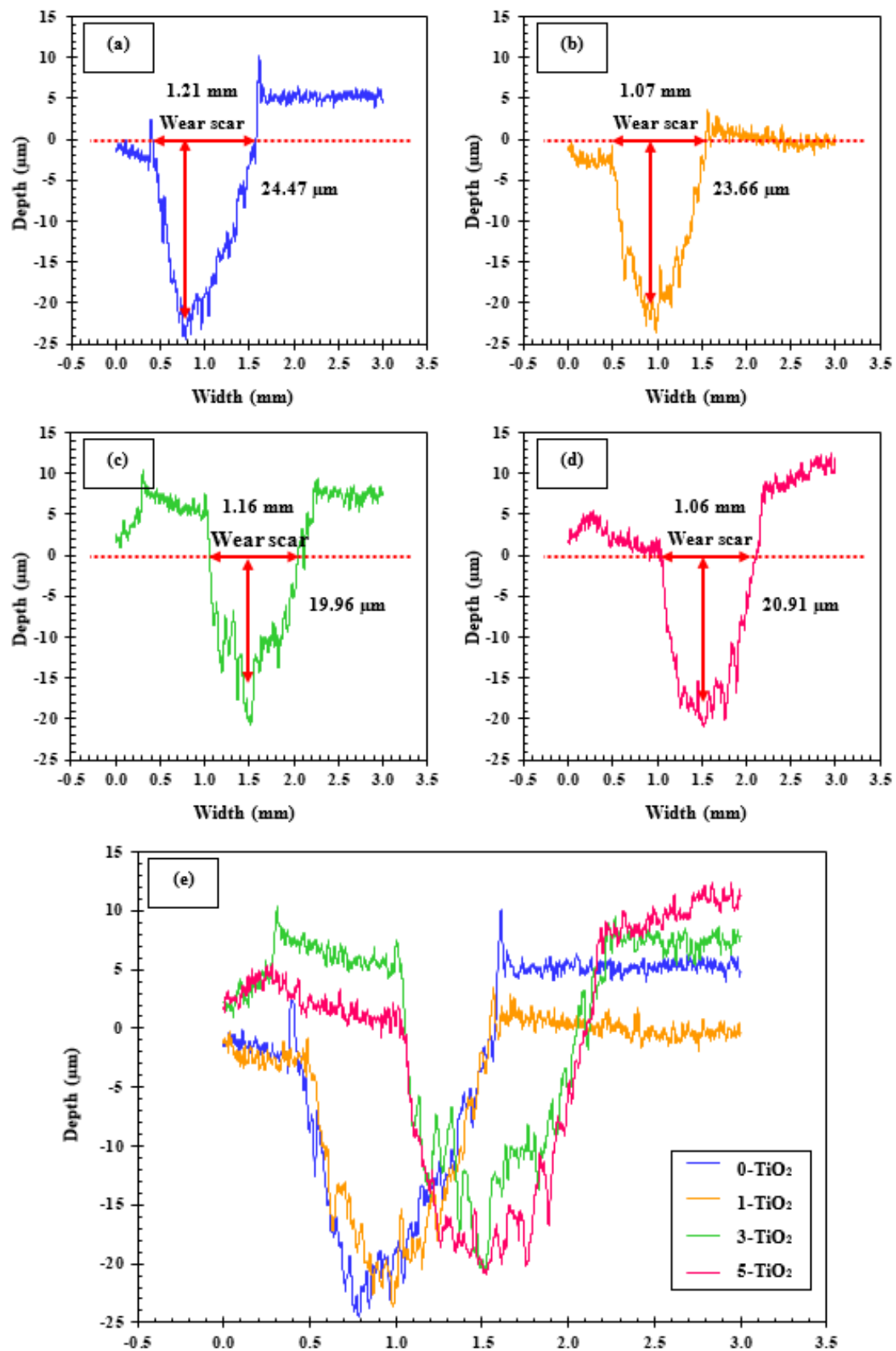


**Figure 8.** The 2D depth profiles of the wear tracks of the specimens (a) without and with (b) 1 g/L, (c) 3 g/L, and (d) 5 g/L of anatase TiO<sub>2</sub> nanoparticles, and (e) overall view of all profiles obtained after the ball-on-disk wear test in SBF solution.



Our results are in good agreement with those of other research works. Improvement in the friction and wear behaviors of PEO coatings after the addition of nanoparticles has also been demonstrated by other researchers. For example, Shokouhfar et al. [18] observed that due to its lowest COF value, despite having a lower surface hardness, a PEO coating with TiO<sub>2</sub> nanoparticles showed a lower wear rate value compared with coatings without nanoparticles or with SiC and Al<sub>2</sub>O<sub>3</sub> nanoparticles. Mozafarnia et al. [30] concluded that increasing the concentration of TiO<sub>2</sub> nanoparticles in the electrolyte up to 3 g/L led to reduced wear weight loss and wear rate values, due to the increase in surface hardness of the PEO coatings. However, further addition of TiO<sub>2</sub> nanoparticles in the electrolyte up to 4 g/L increased the wear weight loss and wear rate values of the coatings, because of the increase in surface roughness and the size of the pores. Aliofkhazraei et al. [20] found that the wear rate of the PEO coatings was reduced by adding CeO<sub>2</sub> nanoparticles into the electrolyte. They reported that the lowest wear rate and the best anti-wear properties were obtained when the concentration of CeO<sub>2</sub> nanoparticles in the electrolyte was 25 g/L. CeO<sub>2</sub> nanoparticles reduced the microstructural defects and surface roughness of the coatings and therefore improved the wear-resistance properties of coatings. However, the wear rate of the coating increased when more CeO<sub>2</sub> nanoparticles up to 50 g/L were embedded into the coating. This might be due to the increasing surface porosity and roughness of coatings caused by the further addition of CeO<sub>2</sub> nanoparticles.

#### 4. Conclusions

In the present study, ceramic porous oxide coatings consisting of anatase and rutile TiO<sub>2</sub> phases were prepared successfully via the plasma electrolytic oxidation (PEO) coating process using the electrolytes with different amounts (0, 1, 3, and 5 g/L) of anatase TiO<sub>2</sub> nanoparticles on pure titanium substrate. The incorporation of TiO<sub>2</sub> nanoparticles into the coatings increased their porosity while decreasing the mean size of the pores and the surface roughness. However, by adding TiO<sub>2</sub> nanoparticles into the electrolyte, no significant effect on the thickness of the coatings was observed. The morphology of worn surfaces after the ball-on-disk wear test in simulated body fluid (SBF) solution indicated plowed grooves parallel to the sliding direction with some detached wear debris, suggesting abrasive wear as the main wear mechanism. Due to their smoother surfaces and the presence of hard TiO<sub>2</sub> nanoparticles on the surfaces and inside the pores, the coatings with TiO<sub>2</sub> nanoparticles showed better wear resistance (lower coefficient of friction and wear rate) than the coating with no TiO<sub>2</sub> nanoparticles. Furthermore, the wear resistance of the TiO<sub>2</sub> nanoparticles-containing coatings increased in the order of 1 g/L < 5 g/L < 3 g/L. The coating with 3 g/L of TiO<sub>2</sub> nanoparticles had the minimum coefficient of friction and wear rate values (0.06 and  $1.33 \times 10^{-6}$  mm<sup>3</sup>/Nm, respectively) and thus the best anti-wear performance in SBF solution. By the addition of 3 g/L of TiO<sub>2</sub> nanoparticles into the electrolyte, the wear rate was reduced by about 32% in comparison to the coating without TiO<sub>2</sub> nanoparticles.

**Author Contributions:** Conceptualization, methodology, writing—review & editing, validation, formal analysis, investigation, M.M.; supervision, conceptualization, methodology, writing—review & editing, A.F.-A.; conceptualization, methodology, writing—review & editing, M.N.; conceptualization, methodology, writing—review & editing, M.K. All authors have read and agreed to the published version of the manuscript.

**Funding:** This research received no external funding.

**Institutional Review Board Statement:** Not applicable.

**Informed Consent Statement:** Not applicable.

**Data Availability Statement:** Data sharing is not applicable.

**Acknowledgments:** We thank Bu-Ali Sina University for financial support to our research group. All the PEO coatings were prepared and electrochemical tests and analysis were performed at A. Fattah-Alhosseini's research laboratories at Bu-Ali Sina University.

**Conflicts of Interest:** The authors declare no conflict of interest.

## References

- Huang, H.L.; Tsai, M.T.; Lin, Y.J.; Chang, Y.Y. Antibacterial and biological characteristics of tantalum oxide coated titanium pretreated by plasma electrolytic oxidation. *Thin Solid Films* **2019**, *688*, 137268. [\[CrossRef\]](#)
- Wang, Y.; Lou, J.; Zeng, L.; Xiang, J.; Zhang, S.; Wang, J.; Xiong, F.; Li, C.; Zhao, Y.; Zhang, R. Osteogenic potential of a novel microarc oxidized coating formed on Ti6Al4V alloys. *Appl. Surf. Sci.* **2017**, *412*, 29–36. [\[CrossRef\]](#)
- Zhang, Y.; Xiu, P.; Jia, Z.; Zhang, T.; Yin, C.; Cheng, Y.; Cai, H.; Zhang, K.; Song, C.; Leng, H.; et al. Effect of vanadium released from micro-arc oxidized porous Ti6Al4V on biocompatibility in orthopedic applications. *Colloids Surf. B Biointerfaces* **2018**, *169*, 366–374. [\[CrossRef\]](#) [\[PubMed\]](#)
- Khan, R.H.U.; Yerokhin, A.L.; Li, X.; Dong, H.; Matthews, A. Influence of current density and electrolyte concentration on DC PEO titania coatings. *Surf. Eng.* **2014**, *30*, 102–108. [\[CrossRef\]](#)
- Fattah-alhosseini, A.; Molaei, M.; Nouri, M.; Babaei, K. Review of the role of graphene and its derivatives in enhancing the performance of plasma electrolytic oxidation coatings on titanium and its alloys. *Appl. Surf. Sci. Adv.* **2021**, *6*, 100140. [\[CrossRef\]](#)
- Shokouhfar, M.; Allahkaram, S.R. Formation mechanism and surface characterization of ceramic composite coatings on pure titanium prepared by micro-arc oxidation in electrolytes containing nanoparticles. *Surf. Coat. Technol.* **2016**, *291*, 396–405. [\[CrossRef\]](#)
- Yazici, S.K.; Muhaffel, F.; Baydogan, M. Effect of incorporating carbon nanotubes into electrolyte on surface morphology of micro arc oxidized Cp-Ti. *Appl. Surf. Sci.* **2014**, *318*, 10–14. [\[CrossRef\]](#)
- Zhang, P.; Wang, X.; Lin, Z.; Lin, H.; Zhang, Z.; Li, W.; Yang, X.; Cui, J. Ti-based biomedical material modified with TiO<sub>x</sub>/TiN<sub>x</sub> duplex bioactivity film via micro-arc oxidation and nitrogen ion implantation. *Nanomaterials* **2017**, *7*, 343. [\[CrossRef\]](#)
- Krzakała, A.; Słuzalska, K.; Dercz, G.; Maciej, A.; Kazez, A.; Szade, J.; Winiarski, A.; Dudek, M.; Michalska, J.; Tylko, G.; et al. Characterisation of bioactive films on Ti-6Al-4V alloy. *Electrochim. Acta* **2013**, *104*, 425–438. [\[CrossRef\]](#)
- Molaei, M.; Fattah-Alhosseini, A.; Gashti, S.O. Sodium aluminate concentration effects on microstructure and corrosion behavior of the plasma electrolytic oxidation coatings on pure titanium. *Metall. Mater. Trans. A Phys. Metall. Mater. Sci.* **2018**, *49*, 368–375. [\[CrossRef\]](#)
- Istrate, B.; Mareci, D.; Munteanu, C.; Stanciu, S.; Luca, D.; Crimu, C.I.; Kamel, E. In vitro electrochemical properties of biodegradable ZrO<sub>2</sub>-CaO coated MgCa alloy using atmospheric plasma spraying. *J. Optoelectron. Adv. Mater.* **2015**, *17*, 1186–1192.
- Nikoomanzari, E.; Fattah-Alhosseini, A.; Karbasi, M.; Nourian, A. A versatile TiO<sub>2</sub>/ZrO<sub>2</sub> nanocomposite coating produced on Ti-6Al-4V via plasma electrolytic oxidation process. *Surf. Interfaces* **2022**, *32*, 102128. [\[CrossRef\]](#)
- Zhang, X.; Cai, G.; Lv, Y.; Wu, Y.; Dong, Z. Growth mechanism of titania on titanium substrate during the early stage of plasma electrolytic oxidation. *Surf. Coat. Technol.* **2020**, *400*, 126202. [\[CrossRef\]](#)
- Garcia-Cabezón, C.; Rodríguez-Mendez, M.L.; Borrás, V.A.; Raquel, B.; Cabello, J.C.R.; Fonseca, A.I.; Martín-Pedrosa, F. Application of plasma electrolytic oxidation coating on powder metallurgy Ti-6Al-4V for dental implants. *Metals* **2020**, *10*, 1167. [\[CrossRef\]](#)
- Yu, J.M.; Kim, H.J.; Ahn, S.G.; Choe, H.C. Plasma electrolytic oxidation of Ti-6Al-4V alloy in electrolytes containing bone formation ions. *Appl. Surf. Sci.* **2020**, *513*, 145776. [\[CrossRef\]](#)
- Molaei, M.; Nouri, M.; Babaei, K.; Fattah-Alhosseini, A. Improving surface features of PEO coatings on titanium and titanium alloys with zirconia particles: A review. *Surf. Interfaces* **2021**, *22*, 100888. [\[CrossRef\]](#)
- Wang, S.; Zhao, Q.; Liu, D.; Du, N. Microstructure and elevated temperature tribological behavior of TiO<sub>2</sub>/Al<sub>2</sub>O<sub>3</sub> composite ceramic coating formed by microarc oxidation of Ti6Al4V alloy. *Surf. Coat. Technol.* **2015**, *272*, 343–349. [\[CrossRef\]](#)
- Shokouhfar, M.; Allahkaram, S.R. Effect of incorporation of nanoparticles with different composition on wear and corrosion behavior of ceramic coatings developed on pure titanium by micro arc oxidation. *Surf. Coat. Technol.* **2017**, *309*, 767–778. [\[CrossRef\]](#)
- Zhou, T.; Ding, Y.; Luo, Q.; Qin, Z.; Zhang, Q.; Shen, B.; Hu, W.; Liu, L. The effects of sodium tungstate on the characteristics of microarc oxidation coating on Ti6Al4V. *J. Mater. Eng. Perform.* **2018**, *27*, 5489–5499. [\[CrossRef\]](#)
- Aliofkhazraei, M.; Gharabagh, R.S.; Teimouri, M.; Ahmadzadeh, M.; Darband, G.B.; Hasannejad, H. Ceria embedded nanocomposite coating fabricated by plasma electrolytic oxidation on titanium. *J. Alloys Compd.* **2016**, *685*, 376–383. [\[CrossRef\]](#)
- Xu, G.; Shen, X. Fabrication of SiO<sub>2</sub> nanoparticles incorporated coating onto titanium substrates by the micro arc oxidation to improve the wear resistance. *Surf. Coat. Technol.* **2019**, *364*, 180–186. [\[CrossRef\]](#)
- Molaei, M.; Fattah-Alhosseini, A.; Nouri, M.; Nourian, A. Systematic optimization of corrosion, bioactivity, and biocompatibility behaviors of calcium-phosphate plasma electrolytic oxidation (PEO) coatings on titanium substrates. *Ceram. Int.* **2022**, *48*, 6322–6337. [\[CrossRef\]](#)
- Kokubo, T.; Takadama, H. How useful is SBF in predicting in vivo bone bioactivity? *Biomaterials* **2006**, *27*, 2907–2915. [\[CrossRef\]](#) [\[PubMed\]](#)



24. Laurindo, C.A.H.; Lepienski, C.M.; Amorim, F.L.; Torres, R.D.; Soares, P. Mechanical and tribological properties of Ca/P-doped titanium dioxide layer produced by plasma electrolytic oxidation: Effects of applied voltage and heat treatment. *Tribol. Trans.* **2018**, *61*, 733–741. [\[CrossRef\]](#)
25. Molaei, M.; Fattah-Alhosseini, A.; Nouri, M.; Mahmoodi, P.; Navard, S.H.; Nourian, A. Enhancing cytocompatibility, antibacterial activity and corrosion resistance of PEO coatings on titanium using incorporated ZrO<sub>2</sub> nanoparticles. *Surf. Interfaces* **2022**, *30*, 101967. [\[CrossRef\]](#)
26. Xie, R.; Lin, N.; Zhou, P.; Zou, J.; Han, P.; Wang, Z.; Tang, B. Surface damage mitigation of TC4 alloy via micro arc oxidation for oil and gas exploitation application: Characterizations of microstructure and evaluations on surface performance. *Appl. Surf. Sci.* **2018**, *436*, 467–476. [\[CrossRef\]](#)
27. Shin, K.R.; Ko, Y.G.; Shin, D.H. Influence of zirconia on biomimetic apatite formation in pure titanium coated via plasma electrolytic oxidation. *Mater. Lett.* **2010**, *64*, 2714–2717. [\[CrossRef\]](#)
28. Molaei, M.; Fattah-Alhosseini, A.; Nouri, M.; Mahmoodi, P.; Nourian, A. Incorporating TiO<sub>2</sub> nanoparticles to enhance corrosion resistance, cytocompatibility, and antibacterial properties of PEO ceramic coatings on titanium. *Ceram. Int.* **2022**, *48*, 21005–21024. [\[CrossRef\]](#)
29. Laurindo, C.A.H.; Bemben, L.M.; Torres, R.D.; Mali, S.A.; Gilbert, J.L.; Soares, P. Influence of the annealing treatment on the tribocorrosion properties of Ca and P containing TiO<sub>2</sub> produced by plasma electrolytic oxidation. *Mater. Technol.* **2016**, *31*, 719–725. [\[CrossRef\]](#)
30. Mozafarnia, H.; Fattah-Alhosseini, A.; Chaharmahali, R.; Nouri, M.; Keshavarz, M.K.; Kaseem, M. Corrosion, wear, and antibacterial behaviors of hydroxyapatite/MgO composite PEO coatings on AZ31 Mg alloy by incorporation of TiO<sub>2</sub> nanoparticles. *Coatings* **2022**, *12*, 1967. [\[CrossRef\]](#)
31. Guo, H.; Liu, Z.; Wang, Y.; Li, J. Tribological mechanism of micro-arc oxidation coatings prepared by different electrolyte systems in artificial seawater. *Ceram. Int.* **2021**, *47*, 7344–7352. [\[CrossRef\]](#)
32. Molaei, M.; Babaei, K.; Fattah-Alhosseini, A. Improving the wear resistance of plasma electrolytic oxidation (PEO) coatings applied on Mg and its alloys under the addition of nano- and micro-sized additives into the electrolytes: A review. *J. Magnes. Alloy.* **2021**, *9*, 1164–1186. [\[CrossRef\]](#)
33. Quintero, D.; Gómez, M.A.; Castaño, J.G.; Tsuji, E.; Aoki, Y.; Echeverría, F.; Habazaki, H. Anodic films obtained on Ti6Al4V in aluminate solutions by spark anodizing: Effect of OH<sup>−</sup> and WO<sub>4</sub><sup>−2</sup> additions on the tribological properties. *Surf. Coat. Technol.* **2017**, *310*, 180–189. [\[CrossRef\]](#)
34. Chen, Z.; Ren, X.; Ren, L.; Wang, T.; Qi, X.; Yang, Y. Improving the tribological properties of spark-anodized titanium by magnetron sputtered diamond-like carbon. *Coatings* **2018**, *8*, 83. [\[CrossRef\]](#)
35. Costa, A.I.; Sousa, L.; Alves, A.C.; Toptan, F. Tribocorrosion behaviour of bio-functionalized porous Ti surfaces obtained by two-step anodic treatment. *Corros. Sci.* **2020**, *166*, 108467. [\[CrossRef\]](#)
36. Aliofkhazraei, M.; Rouhaghdam, A.S. Wear and coating removal mechanism of alumina/titania nanocomposite layer fabricated by plasma electrolysis. *Surf. Coat. Technol.* **2011**, *205*, S57–S62. [\[CrossRef\]](#)

**Disclaimer/Publisher's Note:** The statements, opinions and data contained in all publications are solely those of the individual author(s) and contributor(s) and not of MDPI and/or the editor(s). MDPI and/or the editor(s) disclaim responsibility for any injury to people or property resulting from any ideas, methods, instructions or products referred to in the content.